JCIM JOURNAL OF CHEMICAL INFORMATION AND MODELING

Article

Cite This: J. Chem. Inf. Model. 2019, 59, 2165−2174

pubs.acs.org/jcim

Quasiclassical Correlation Functions from the Wigner Density Using the Stability Matrix

Amartya Bose[†] and Nancy Makri*[,†,‡]

[†]Department of Chemistry, University of Illinois, 505 S. Mathews Avenue, Urbana, Illinois 61801, United States

[‡]Department of Physics, University of Illinois, 1110 W. Green Street, Urbana, Illinois 61801, United States

ABSTRACT: Accounting for zero-point energy in the initial conditions of classical trajectory calculations of time correlation functions requires sampling from a quantized phase space distribution, which is often chosen as the Weyl−Wigner transform of a thermalized operator. The numerical construction of the latter and its use as a sampling function can be challenging. We show that the operator dependence of the phase space distribution can be transferred to the dynamics, allowing sampling from the simpler Wigner phase space density. The method involves augmenting the classical equations of motion with additional differential equations for elements of the stability matrix. We also propose a local harmonic approximation for the dynamical derivatives, which significantly reduces the computational cost required to obtain correlation functions of nonlinear operators. We illustrate the method with application to linear and nonlinear correlation functions of model Hamiltonians. While the local harmonic approximation is not always successful in predicting nonlinear correlation functions of one degree of freedom, it quantitatively captures the full quasiclassical results for systems in contact with dissipative environments.

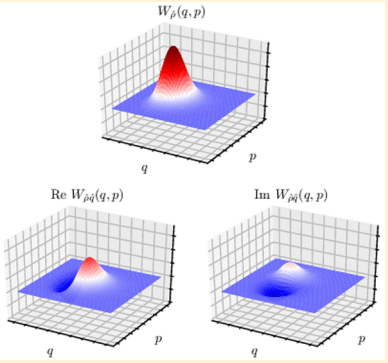

1. INTRODUCTION

While the quest for efficient quantum mechanical methods continues with unprecedented intensity in the theoretical chemistry community, classical mechanics often provides an appealing alternative and remains the method of choice for the simulation of many dynamical processes in condensed phase and biological systems. Classical trajectory methods are ideally suited to systems described by continuous coordinates whose dynamics is governed by single Born−Oppenheimer potential surfaces or force fields, where the large number of degrees of freedom is expected to wash out quantum interference effects at sufficiently high temperatures such that quantum mechanical tunneling does not play an important role. Under such conditions, the only quantum mechanical effect that needs to be accounted for is zero-point energy (ZPE). The latter manifests itself as a broadening of the Boltzmann distribution and has severe consequences on the potential regions accessible by classical trajectories.

To include ZPE effects in the thermal distribution from which classical trajectories are sampled, one needs to be able to compute the Boltzmann density and transform it to a phase space function. Because position and momentum are complementary variables in quantum mechanics, such a transformation is not unique. The most common prescriptions for constructing quantized phase space distributions are the Husimi transform,[1] which employs coherent states and is used in forward−backward semiclassical dynamics[2−4] (FBSD) and the forward−backward initial value representation[5−7] (FB-IVR), and the Weyl−Wigner transform[8,9] of an operator, which involves a Fourier-type integral,

$$W_O(\mathbf{q},\mathbf{p}) = (2\pi\hbar)^{n/2}\int \mathrm{d}\xi \left\langle \mathbf{q}+\frac{1}{2}\xi\middle|\hat{O}\middle|\mathbf{q}-\frac{1}{2}\xi\right\rangle \mathrm{e}^{-i\mathbf{p}\cdot\xi/\hbar} \tag{1.1}$$

(where n is the number of degrees of freedom). The Weyl−Wigner phase space transform is used in quasiclassical calculations according to the "Wigner prescription",[9,10] which is equivalent to the linearized semiclassical initial value representation[11−13] (LSC-IVR) and the linearized path integral[14] (LPI).

Consider a quantum mechanical correlation function of two operators $\hat{A}$ and $\hat{B}$,

$$C_{AB}^{\mathrm{QM}}(t) = \mathrm{Tr}(\hat{\rho}_0\hat{A}\hat{B}(t)) \tag{1.2}$$

where we assume that the operators are functions of position coordinates. The Wigner-based quasiclassical approximation to eq 1.2 is given by the expression[9]

$$C_{AB}(t) = \int_{-\infty}^{\infty}\mathrm{d}\mathbf{q}_0\int_{-\infty}^{\infty}\mathrm{d}\mathbf{p}_0 W_{\rho_0 A}(\mathbf{q}_0,\mathbf{p}_0)B(\mathbf{q}_t) \tag{1.3}$$

where $\mathbf{q}_0,\mathbf{p}_0$ are phase space variables that specify the initial condition of a classical trajectory that reaches the phase space coordinates $\mathbf{q}_t,\mathbf{p}_t$ at the time t, and $W_{\rho_0 A}$ is the Weyl−Wigner transform of the operator $\hat{\rho}_0\hat{A}$. Equation 1.3 requires selection by Monte Carlo[15] of phase space points from $W_{\rho_0 A}$ or a function closely related to that. For this purpose, the Weyl−Wigner

Special Issue: Women in Computational Chemistry

Received: January 24, 2019
Published: February 26, 2019

DOI: 10.1021/acs.jcim.9b00081
J. Chem. Inf. Model. 2019, 59, 2165−2174

transform of $\hat{\rho}_0\hat{A}$ must be available or easy to generate and should give rise to a convenient sampling function.

Unfortunately, the multidimensional Fourier-type integral in eq 1.1 makes the Weyl−Wigner transform extremely difficult to compute in systems of many degrees of freedom. (This difficulty is the main appeal of FBSD/FB-IVR methods as an alternative to Wigner dynamics.) Several methods have been developed for obtaining the Wigner phase space density W_{ρ_0} for the bare Boltzmann operator $\hat{\rho}_0 = Z^{-1}\exp(-\beta\hat{H})$. These include local[16] or variationally optimized[14] Gaussian wavepacket approaches and the thermal Gaussian approximation[17,18] (which employ frozen Gaussian dynamics[19] in imaginary time), along with extensions that capture quantum corrections.[20] We recently introduced the adiabatic switching Wigner (ASW) method,[21,22] a simple trajectory-based procedure that makes use of the classical adiabatic theorem to slowly convert the Wigner density of a harmonic reference system to that of the target Hamiltonian. Other recent work[23] has used the quasi-adiabatic propagator path integral methodology[24] to obtain the Wigner distribution of the bath in the case of a system interacting with a bath of independent harmonic oscillators. Last, we have recently developed a coherent state based path integral method for constructing the Wigner function[25] (CSPIW), a numerically exact procedure for transforming the Husimi density to the Wigner distribution, which circumvents the numerical difficulties associated the oscillatory Wigner integral.

The Wigner−Weyl transform, $W_{\rho_0 A}$, for a linear operator, along with the bare Wigner density, W_{ρ_0}, are shown in Figure 1

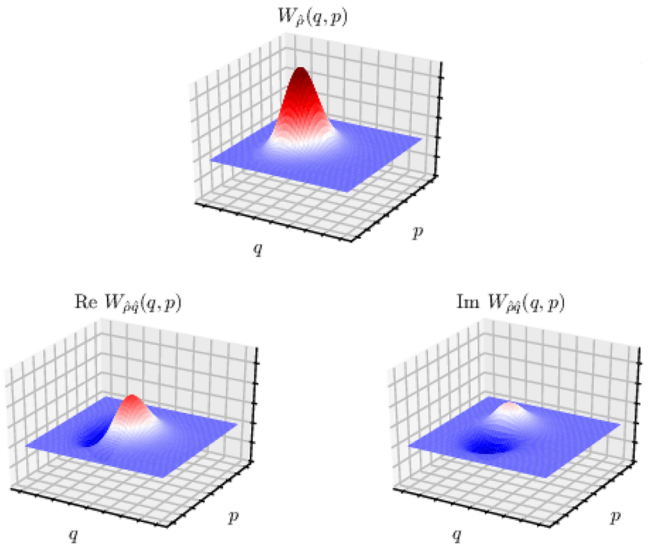

Figure 1. Wigner density W_ρ for the Boltzmann operator and the Weyl−Wigner transform $W_{\rho A}$ for $\hat{A} = \hat{q}$ for the one-dimensional anharmonic potential described in section 4.

for the anharmonic system employed in section 4. It is seen that $W_{\rho_0 A}$ is complex-valued with large negative components, so its absolute value must be used to construct a Monte Carlo sampling function, in contrast to the Wigner density W_{ρ_0} which is real and at finite temperatures, often, non-negative. More importantly, constructing the Weyl−Wigner function, $W_{\rho_0 A}$, often presents a more challenging task. To circumvent these difficulties, the operator $\hat{A}$ is sometimes moved outside of the Weyl−Wigner function, giving rise to the approximate expression

$$C_{AB}(t) \simeq \int_{-\infty}^{\infty} d\mathbf{q}_0 \int_{-\infty}^{\infty} d\mathbf{p}_0 W_{\rho_0}(\mathbf{q}_0, \mathbf{p}_0) A(\mathbf{q}_0) B(\mathbf{q}_t) \tag{1.4}$$

Eq 1.4 is *an approximation* to the quasiclassical correlation function, eq 1.3. It is obvious that this expression is real-valued, so it cannot account for the imaginary part of quantum correlation functions, which leads to asymmetry in frequency space; thus it is extremely important for extracting spectra. The real part of the correlation function predicted by eq 1.4 is also approximate in most situations. Thus, the proper calculation of a quasiclassical correlation function must be based on eq 1.3.

The goal of this paper is to transfer the operator dependence of the initial distribution to the dynamics. In section 2, we describe an approach that achieves this goal, obtaining an expression that is exactly equivalent to eq 1.3 but requires knowledge of the Wigner transform of the bare density operator. The proposed method can be used in conjunction with any (exact or approximate) method for generating the Wigner density. In section 3, we develop a procedure for obtaining the required dynamical derivatives, utilizing the equation of motion of the classical stability matrix. In the same section, we also propose a local harmonic approximation that simplifies the computation of higher order derivatives. We illustrate the procedure in sections 4 and 5 with applications to correlation functions of linear and nonlinear operators in a model of one degree of freedom and also in a system-bath Hamiltonian. In section 6, we give some concluding remarks on the utility of the approach.

2. QUASICLASSICAL TIME CORRELATION FUNCTION IN TERMS OF WIGNER DENSITY

For clarity, we first consider a system of a single degree of freedom. Since the operator $\hat{A}$ is assumed local in position space, the Weyl−Wigner transform becomes

$$W_{\rho_0 A}(q,p) = (2\pi\hbar)^{-(n/2)} \int d\xi \left\langle q + \frac{1}{2}\xi \middle| \hat{\rho}_0 \middle| q - \frac{1}{2}\xi \right\rangle A\left(q - \frac{1}{2}\xi\right) e^{-ip\xi/\hbar} \tag{2.1}$$

To proceed, we expand the operator $\hat{A}(q)$ in a Taylor series,

$$W_{\rho_0 A}(q,p) = (2\pi\hbar)^{-(n/2)} \sum_{k=0}^{\infty} \frac{1}{k!}(-2)^{-k}\left(\frac{\partial^k A}{\partial q^k}\right) \int d\xi \left\langle x + \frac{1}{2}\xi \middle| \hat{\rho}_0 \middle| x - \frac{1}{2}\xi \right\rangle \xi^k e^{-ip\xi/\hbar} \tag{2.2}$$

Noting that the ξ powers amount to momentum derivatives leads to the form

$$W_{\rho_0 A}(q,p) = \sum_{k=0}^{\infty} \frac{1}{k!}\left(-\frac{1}{2}i\hbar\right)^k \left(\frac{\partial^k A}{\partial q^k}\right)\left(\frac{\partial^k W_{\rho_0}}{\partial p^k}\right) \tag{2.3}$$

Using eq 2.3, the quasiclassical correlation function becomes

DOI: 10.1021/acs.jcim.9b00081
J. Chem. Inf. Model. 2019, 59, 2165−2174

$$C_{AB}(t) = \int_{-\infty}^{\infty} dq_0 \int_{-\infty}^{\infty} dp_0 \sum_{k=0}^{\infty} \frac{1}{k!}\left(-\frac{1}{2}i\hbar\right)^k \frac{\partial^k W_{\rho_0}(q_0, p_0)}{\partial {p_0}^k} \frac{\partial^k A(q_0)}{\partial {q_0}^k} B(q_t) \tag{2.4}$$

Using repeated integration by parts, the momentum derivatives of the thermal Wigner function can be transferred to the factor $B(q_t)$, which depends implicitly on the initial momentum value p_0:

$$C_{AB}(t) = \int_{-\infty}^{\infty} dq_0 \int_{-\infty}^{\infty} dp_0 \sum_{k=0}^{\infty} \frac{1}{k!}\left(\frac{1}{2}i\hbar\right)^k W_{\rho_0}(q_0, p_0) \frac{\partial^k A(q_0)}{\partial {q_0}^k} \frac{\partial^k B(q_t)}{\partial {p_0}^k} \tag{2.5}$$

Equation 2.5 has the desired form. Trajectory initial conditions are now sampled from the bare Wigner density, which may be available or evaluated on the fly. The required momentum derivatives of $B(q_t)$ are converted to derivatives with respect to q_t using the chain rule. The procedure required to calculate these derivatives is discussed in the next section.

It is straightforward to extend the above procedure to systems of many degrees of freedom. The Weyl−Wigner transform of the desired operator becomes

$$\begin{aligned} W_{\rho_0 A}(\mathbf{q}, \mathbf{p}) &= \sum_{k=0}^{\infty} \frac{1}{k!}\left(-\frac{1}{2}i\hbar\right)^k \sum_{\{j_m\}} \frac{k!}{j_1!j_2!\cdots j_n!} \frac{\partial^k A}{\prod_l \partial {q_l}^{j_l}} \frac{\partial^k}{\prod_{l'} \partial {p_{l'}}^{j_{l'}}} W_{\rho_0}(\mathbf{q}, \mathbf{p}) \\ &= \sum_{k=0}^{\infty} \frac{1}{k!}\left(-\frac{1}{2}i\hbar\right)^k \sum_{\{j_m\}} \frac{k!}{j_1!j_2!\cdots j_m!} \partial_{\mathbf{p}}^{\{j_m\}} W_{\rho_0}(\mathbf{q}, \mathbf{p}) \partial_{\mathbf{q}}^{\{j_m\}} A(\mathbf{q}) \end{aligned} \tag{2.6}$$

where $\{j_m\}$ represents a positive semidefinite ordered n-tuple such that $\sum_{m=1}^{n} j_m = k$, and

$$\partial_{\mathbf{q}}^{\{j_m\}} \equiv \frac{\partial^k}{\prod_l \partial {q_l}^{j_l}}, \qquad \partial_{\mathbf{p}}^{\{j_m\}} \equiv \frac{\partial^k}{\prod_l \partial {p_l}^{j_l}} \tag{2.7}$$

After incorporating eq 2.6 in the expression and carrying out the repeated integration by parts, the correlation function becomes

$$C_{AB}(t) = \int_{-\infty}^{\infty} d\mathbf{q}_0 \int_{-\infty}^{\infty} d\mathbf{p}_0 \sum_{k=0}^{\infty} \frac{1}{k!}\left(\frac{1}{2}i\hbar\right)^k \sum_{\{j_m\}} \frac{k!}{j_1!j_2!\cdots j_m!} W_{\rho_0}(\mathbf{q}_0, \mathbf{p}_0) \partial_{\mathbf{q}_0}^{\{j_m\}} A(\mathbf{q}_0) \partial_{\mathbf{p}_0}^{\{j_m\}} B(\mathbf{q}_t) \tag{2.8}$$

Again, the derivatives of $B(\mathbf{q}_t)$ are evaluated via the chain rule.

Equation 2.8 is the main result of this paper. We emphasize that no approximations have been introduced, so eq 2.8 is exactly equivalent to eq 1.3. As such, it accounts for the imaginary part of quantum correlation functions (even within the quasiclassical treatment of the dynamics), yet the phase space density is simply the Wigner thermal distribution, which is easier to evaluate and independent of the particular form of the operator $\hat{A}$.

We note that the infinite sum that appears in eq 2.5 truncates rapidly if $\hat{B}$ is a low-order polynomial, as is frequently the case in the evaluation of dipole moment correlation functions. For example, this sum reduces to a single term in the case of linear operators.

In the next section, we explore the structure of eq 2.8 and propose a simplification that greatly speeds up its evaluation in the case of nonlinear operators.

3. DERIVATIVE EVALUATION AND LOCAL HARMONIC APPROXIMATION

In this section, we discuss the evaluation of the momentum derivatives that appear in eq 2.8. For clarity, we consider again a system of one degree of freedom described by the Hamiltonian

$$\hat{H} = \frac{\hat{p}^2}{2m} + V(\hat{q}) \tag{3.1}$$

We begin by writing out eq 2.5 explicitly, evaluating the derivatives with respect to p_0 via the chain rule:

$$\begin{aligned} C_{AB}(t) = \int_{-\infty}^{\infty} dq_0 \int_{-\infty}^{\infty} dp_0 W_{\rho_0}(q_0, p_0) \Bigg\{ & A(q_0)B(q_t) \\ & + \frac{1}{2}i\hbar A'(q_0)\frac{\partial q_t}{\partial p_0}B'(q_t) + \frac{1}{2!}\left(\frac{1}{2}i\hbar\right)^2 A''(q_0) \\ & \left(\frac{\partial^2 q_t}{\partial {p_0}^2}B'(q_t) + \left(\frac{\partial q_t}{\partial p_0}\right)^2 B''(q_t)\right) + \frac{1}{3!}\left(\frac{1}{2}i\hbar\right)^3 \\ & A'''(q_0)\left(\frac{\partial^3 q_t}{\partial {p_0}^3}B'(q_t) + 3\frac{\partial q_t}{\partial p_0}\frac{\partial^2 q_t}{\partial {p_0}^2}B''(q_t) \right. \\ & \left. + \left(\frac{\partial q_t}{\partial p_0}\right)^3 B'''(q_t)\right) + \cdots \Bigg\} \end{aligned} \tag{3.2}$$

The derivative $\partial q_t/\partial p_0$ in the right-hand side of eq 3.2 is an element of the trajectory stability matrix,

$$\mathbf{T}_t = \begin{pmatrix} \frac{\partial q_t}{\partial q_0} & \frac{\partial q_t}{\partial p_0} \\ \frac{\partial p_t}{\partial q_0} & \frac{\partial p_t}{\partial p_0} \end{pmatrix} \tag{3.3}$$

which is known to satisfy the differential equation

$$\frac{d}{dt}\mathbf{T}_t = \mathbf{K}_t \cdot \mathbf{T}_t \tag{3.4}$$

where

$$\mathbf{K}_t = \begin{pmatrix} 0 & m^{-1} \\ -V''(q_t) & 0 \end{pmatrix} \tag{3.5}$$

and the initial condition for $\mathbf{T}_t$ is the identity matrix. Since we are only interested in the $\partial/\partial p_0$ derivative, we do not need to solve the equations for the entire stability matrix. Instead, the desired derivative is obtained by integrating the following pair of coupled differential equations,

DOI: 10.1021/acs.jcim.9b00081
J. Chem. Inf. Model. 2019, 59, 2165−2174

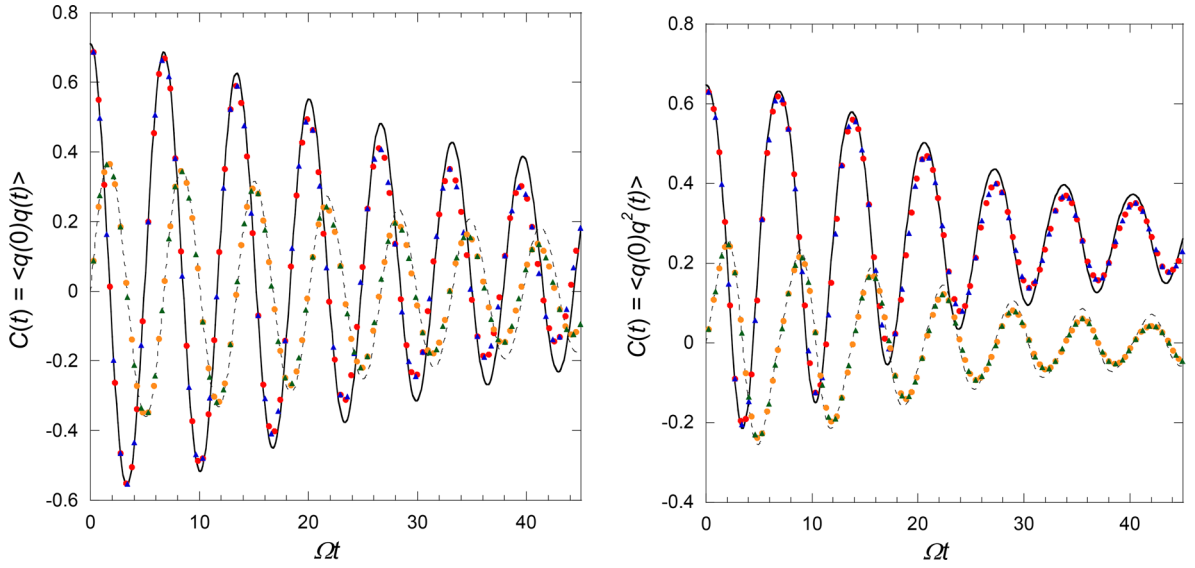

Figure 2. Correlation functions for the anharmonic oscillator with $A = q$. Solid black line, real part of basis set calculation. Dotted black line, imaginary part of basis set calculation. Red circles, real part of full quasiclassical correlation. Blue triangles, imaginary part of full quasiclassical correlation. Orange circles, real part of LHA correlation function. Green triangles, imaginary part of LHA correlation function. Left, $B = q$. Right, $B = q^2$.

$$\frac{\mathrm{d}}{\mathrm{d}t}\frac{\partial q_t}{\partial p_0} = \frac{1}{m}\frac{\partial p_t}{\partial p_0}$$
$$\frac{\mathrm{d}}{\mathrm{d}t}\frac{\partial p_t}{\partial p_0} = -V''(q_t)\frac{\partial q_t}{\partial p_0} \tag{3.6}$$

with initial conditions 0 and 1, respectively. The higher order derivatives are obtained by differentiating eqs 3.6 with respect to p_0:

$$\frac{\mathrm{d}}{\mathrm{d}t}\frac{\partial^2 q_t}{\partial {p_0}^2} = \frac{1}{m}\frac{\partial^2 p_t}{\partial {p_0}^2}$$
$$\frac{\mathrm{d}}{\mathrm{d}t}\frac{\partial^2 p_t}{\partial {p_0}^2} = -V'''(q_t)\left(\frac{\partial q_t}{\partial p_0}\right)^2 - V''(q_t)\frac{\partial^2 q_t}{\partial {p_0}^2} \tag{3.7}$$

$$\frac{\mathrm{d}}{\mathrm{d}t}\frac{\partial^3 q_t}{\partial {p_0}^3} = \frac{1}{m}\frac{\partial^3 p_t}{\partial {p_0}^3}$$
$$\frac{\mathrm{d}}{\mathrm{d}t}\frac{\partial^3 p_t}{\partial {p_0}^3} = -V^{(iv)}(q_t)\left(\frac{\partial q_t}{\partial p_0}\right)^3 - 3V'''(q_t)\frac{\partial q_t}{\partial p_0}\frac{\partial^2 q_t}{\partial {p_0}^2} - V''(q_t)\frac{\partial^3 q_t}{\partial {p_0}^3} \tag{3.8}$$

etc., with initial conditions equal to zero.

It is straightforward to extend these expressions to systems with many degrees of freedom. However, we note that the computational cost of calculating and storing the higher order derivatives of the potential energy surface beyond the Hessian grows quickly. To address this issue, we propose a local harmonic approximation (LHA) where we set all derivatives of the potential beyond the second to zero. It can be shown that the LHA is equivalent to ignoring all terms involving higher order derivatives of the stability matrix, consequently simplifying eq 3.2 to

$$C_{AB}(t) = \int_{-\infty}^{\infty}\mathrm{d}q_0\int_{-\infty}^{\infty}\mathrm{d}p_0 W_{\rho_0}(q_0, p_0)\left\{A(q_0)B(q_t) + \frac{1}{2}i\hbar A'(q_0)\frac{\partial q_t}{\partial p_0}B'(q_t) + \frac{1}{2!}\left(\frac{1}{2}i\hbar\right)^2 A''(q_0)\left(\frac{\partial q_t}{\partial p_0}\right)^2 B''(q_t) + \frac{1}{3!}\left(\frac{1}{2}i\hbar\right)^3 A'''(q_0)\left(\frac{\partial q_t}{\partial p_0}\right)^3 B'''(q_t) + \cdots\right\} \tag{3.9}$$

Note that in the case of a linear $\hat{A}$, eq 3.9 is identical to eq 3.2, that is, the LHA yields the exact quasiclassical correlation function. For a quadratic $\hat{A}$, the real part of the correlation function under LHA no longer equals the full quasiclassical result, but the imaginary part is still treated exactly. From operators of order higher than quadratic, both the real and the imaginary part obtained via the LHA become approximate.

In the next two sections, we illustrate the features of the approach and the accuracy of the LHA approximation with applications to a one-dimensional model and a system-bath Hamiltonian. In all cases, the density is given by the Boltzmann operator, that is, $\hat{\rho}_0 = Z^{-1}\exp(-\beta\hat{H})$.

4. APPLICATION TO AN ANHARMONIC OSCILLATOR

In this section, we apply the method to a strongly anharmonic system with Hamiltonian

$$\hat{H} = \frac{\hat{p}^2}{2} + \frac{1}{2}\Omega^2\hat{q}^2 - 0.2\hat{q}^3 + 0.015\hat{q}^4 \tag{4.1}$$

where $\Omega = \sqrt{2}$. We report various correlation functions (using both the full equations and LHA) and their comparisons with fully quantum mechanical basis set results at a temperature that corresponds to $\hbar\Omega\beta = \sqrt{2}$. The initial Wigner distribution was obtained via the CSPIW approach,[25] which converged with $n_x = 3$ and $n_p = 4$.

We begin by examining correlation functions where $\hat{A} = \hat{q}$. Figure 2 shows the autocorrelation function ($\hat{B} = \hat{q}$), as well as the mixed correlation function with a quadratic operator ($\hat{B} =$

DOI: 10.1021/acs.jcim.9b00081
J. Chem. Inf. Model. 2019, 59, 2165−2174

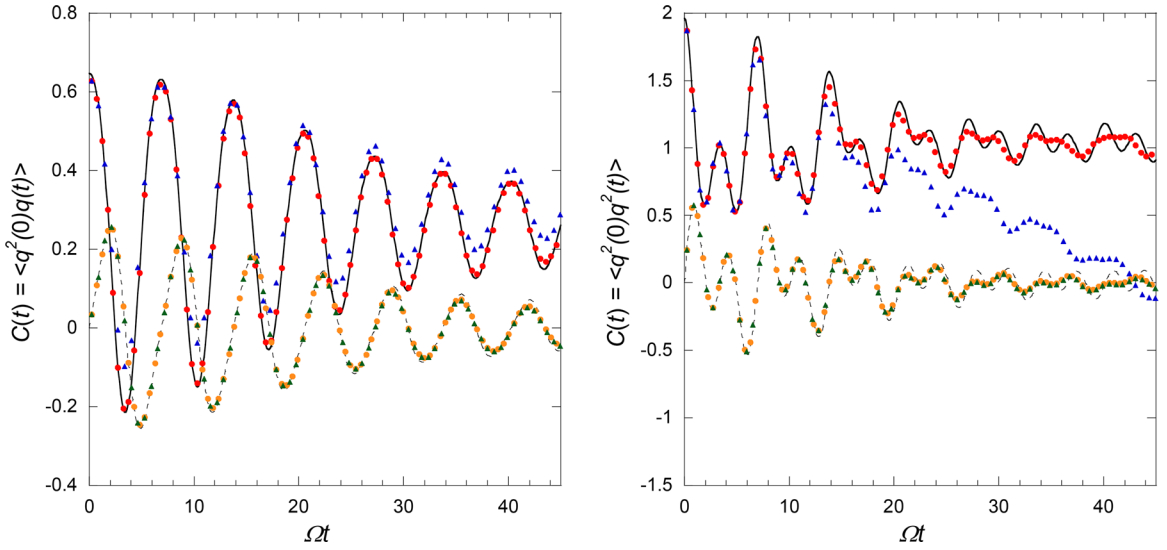

Figure 3. Correlation functions for the anharmonic oscillator with $A = q^2$. Solid black line, real part of basis set calculation. Dotted black line, imaginary part of basis set calculation. Red circles, real part of full quasiclassical correlation. Blue triangles, imaginary part of full quasiclassical correlation. Orange circles, real part of LHA correlation function. Green triangles, imaginary part of LHA correlation function. Left, $B = q$. Right, $B = q^2$.

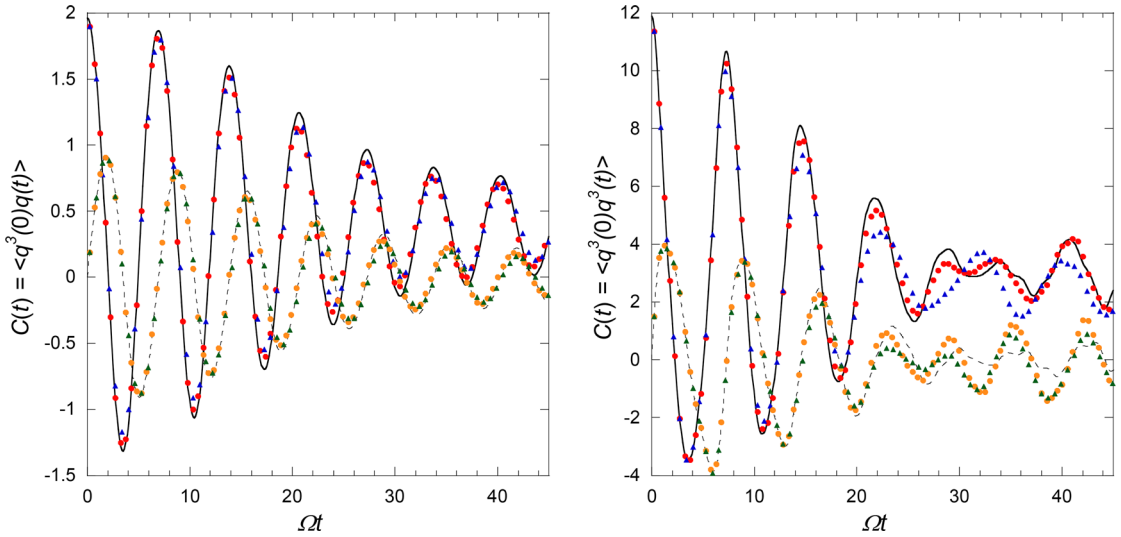

Figure 4. Correlation functions for the anharmonic oscillator with $\hat{A} = q^3$. Solid black line, real part of basis set calculation. Dotted black line, imaginary part of basis set calculation. Red circles, real part of full quasiclassical correlation. Blue triangles, imaginary part of full quasiclassical correlation. Orange circles, real part of LHA correlation function. Green triangles, imaginary part of LHA correlation function. Left, $B = q$. Right, $B = q^3$.

$\hat{q}^2$). The quasiclassical trajectory results are in good agreement with the numerically exact basis set results, although (as expected) the quasiclassical approximation dephases slightly faster and is unable to account for the rephasing that the quantum correlation function would display at longer times. Because of the linear form of the first operator, the LHA results are in quantitative agreement with the full quasiclassical results.

In Figure 3, we show correlation functions for $\hat{A} = \hat{q}^2$, for a linear and a quadratic second operator. Overall, the full quasiclassical correlation function is in good agreement with the basis set results. In both cases, the imaginary part of the LHA correlation function matches quantitatively the full quasiclassical correlation function, in line with the discussion in section 3. The LHA approximation leads to small errors in the real part in the case $\hat{B} = \hat{q}$, and predicts a flawed monotonic decrease of the correlation function for $\hat{B} = \hat{q}^2$.

Last, we consider correlation functions with $\hat{A} = \hat{q}^3$. Figure 4 shows the correlation functions for $\hat{B} = \hat{q}$ and for $\hat{B} = \hat{q}^3$. The full quasiclassical results provide a very good approximation to the quantum correlation functions in this case, and are able to capture many of their subtle features. In this case, the LHA treatment is approximate both for the real and for the imaginary part of the quasiclassical correlation functions. For the linear second operator, the LHA results are seen to be quantitative, while small errors are visible in the other case. The LHA approximation does not lead to large errors in this case.

The results shown in Figures 2−4 indicate that the quasiclassical approximation, with proper quantization of trajectory initial conditions, reproduces the quantum mechanical correlation functions of position operators rather well prior to the onset of quantum rephasing. While this behavior is well established, we point out that this trend seems to persist for correlation functions of highly nonlinear operators. The method

DOI: 10.1021/acs.jcim.9b00081
J. Chem. Inf. Model. 2019, 59, 2165−2174

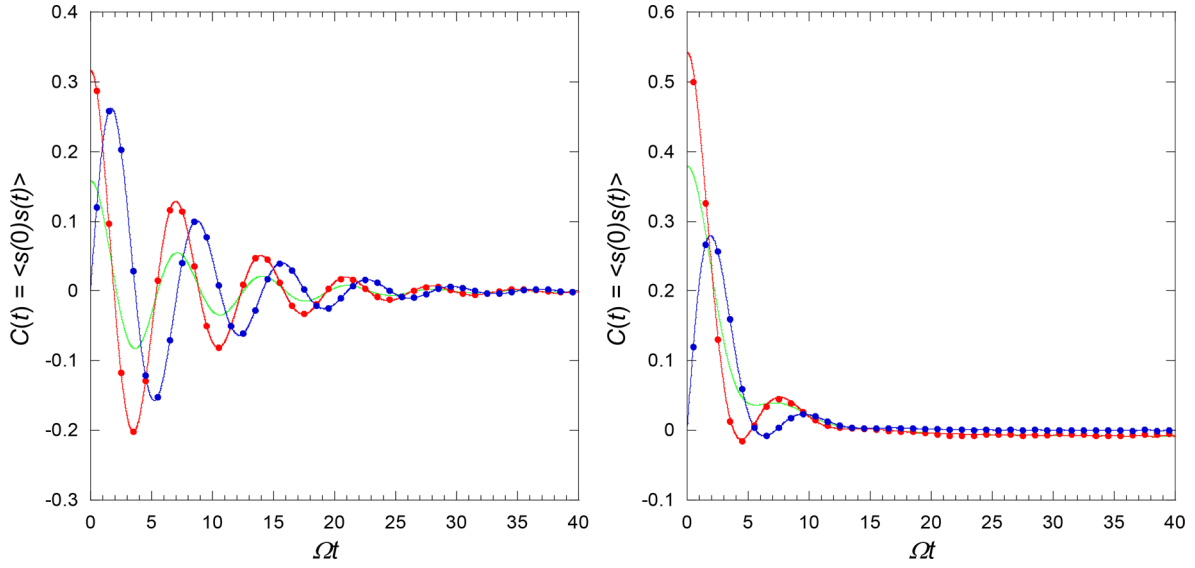

Figure 5. Position autocorrelation functions of a harmonic system coupled to a harmonic bath. Solid red line, real part of exact quantum correlation function. Solid blue line, imaginary part of exact quantum correlation function. Red markers, real part of quasiclassical correlation. Blue markers, imaginary part of quasiclassical correlation. Green solid line, classical correlation function. $\hbar\Omega\beta = 5$. Left, $\xi = 0.6$. Right, $\xi = 1.2$.

presented in section 2 allows the full evaluation of a quasiclassical correlation function (including its imaginary part) using the Wigner function obtained solely from the density operator. The LHA treatment greatly simplifies the approach and leads to exact results if the first operator is linear. When the first operator is nonlinear, our calculations showed that the LHA approximation can be rather good but can also fail.

One-dimensional models are most challenging for quasiclassical approximations, where quantum phase coherence and wavepacket revival is most dramatic. These delicate quantum effects tend to be washed out in systems of many degrees of freedom, and thus such systems can be more forgiving to quasiclassical treatments, as long as ZPE effects are accounted for. We thus proceed to examine in the next section a multidimensional model.

5. SYSTEM-BATH DYNAMICS

Last, we demonstrate the approach on a system, described by the coordinate s, that is coupled to a harmonic bath according to the Hamiltonian

$$\hat{H} = \frac{1}{2}\hat{p}^2 + V_0(\hat{s}) + \sum_{j=1}^{n}\left(\frac{1}{2}\hat{P}_j^2 + \frac{1}{2}\omega_j^2\hat{Q}_j^2 - c_j\hat{s}\hat{Q}_j\right) \tag{5.1}$$

The frequencies and the couplings of the harmonic bath are specified by the spectral density function.[26] In this paper, we use the Ohmic form with an exponential cutoff,

$$J(\omega) = \frac{\pi}{2}\hbar\xi\omega\, e^{-\omega/\omega_c} \tag{5.2}$$

with $\omega_c = 1.25\Omega$. The spectral density was discretized into $n = 60$ bath modes using the logarithmic discretization scheme[27,28] with $\omega_{max} = 4\omega_c$.

We monitor correlation functions of operators that depend on the system position, for which eq 2.8 becomes

$$C_{AB}(t) = \int ds_0 \int dp_0 \int d\mathbf{Q}_0 \int d\mathbf{P}_0 W_{\rho_0}(s_0, p_0, \mathbf{Q}_0, \mathbf{P}_0)$$
$$\left\{A(s_0)B(s_t) + \frac{1}{2}i\hbar A'(q_0)\frac{\partial s_t}{\partial p_0}B'(s_t) + \frac{1}{2!}\left(\frac{1}{2}i\hbar\right)^2\right.$$
$$A''(s_0)\left(\frac{\partial^2 s_t}{\partial p_0^2}B'(s_t) + \left(\frac{\partial s_t}{\partial p_0}\right)^2 B''(s_t)\right)$$
$$+ \frac{1}{3!}\left(\frac{1}{2}i\hbar\right)^3 A'''(s_0)\left(\frac{\partial^3 s_t}{\partial p_0^3}B'(s_t)\right.$$
$$\left.\left. + 3\frac{\partial s_t}{\partial p_0}\frac{\partial^2 s_t}{\partial p_0^2}B''(s_t) + \left(\frac{\partial s_t}{\partial p_0}\right)^3 B'''(s_t)\right) + \cdots\right\} \tag{5.3}$$

The differential equations for the trajectory derivatives are given in the Appendix. These equations, along with the zero initial conditions, imply that (just as in the case of a single degree of freedom) all the higher order derivatives of the stability matrix are identically zero at all times in the LHA. Thus, the correlation function under the LHA becomes

$$C_{AB}(t) \simeq \int ds_0 \int dp_0 \int d\mathbf{Q}_0 \int d\mathbf{P}_0 W_{\rho_0}(s_0, p_0, \mathbf{Q}_0, \mathbf{P}_0)$$
$$\left\{A(s_0)B(s_t) + \frac{1}{2}i\hbar A'(q_0)\frac{\partial s_t}{\partial p_0}B'(s_t) + \frac{1}{2!}\left(\frac{1}{2}i\hbar\right)^2\right.$$
$$A''(s_0)\left(\frac{\partial s_t}{\partial p_0}\right)^2 B''(s_t) + \frac{1}{3!}\left(\frac{1}{2}i\hbar\right)^3 A'''(s_0)\left(\frac{\partial s_t}{\partial p_0}\right)^3$$
$$\left. B'''(s_t) + \cdots\right\} \tag{5.4}$$

Below we apply these expressions to two system potentials.

DOI: 10.1021/acs.jcim.9b00081
J. Chem. Inf. Model. 2019, 59, 2165−2174

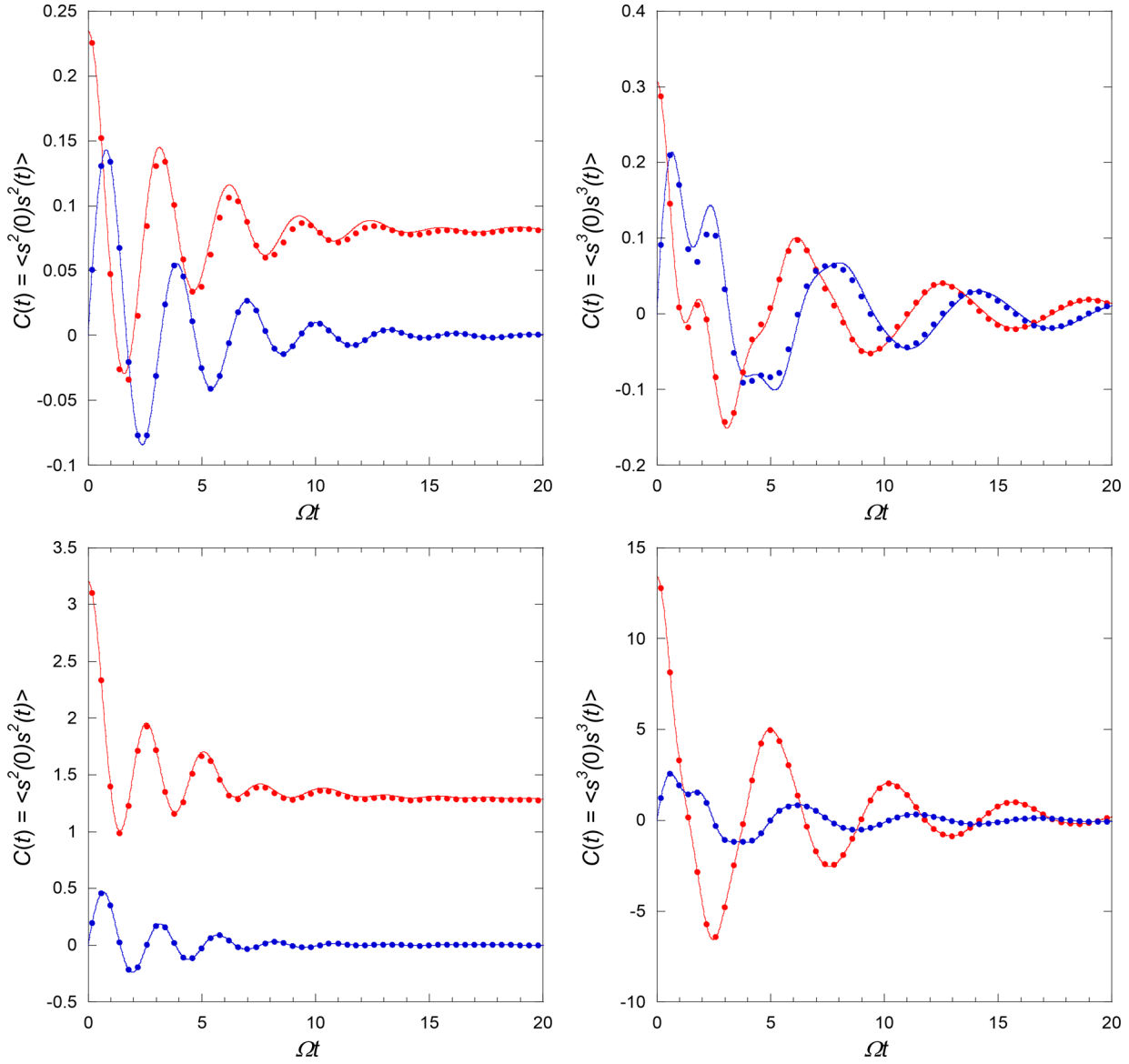

Figure 6. Correlation functions of anharmonic system coupled to a harmonic bath. The red and blue lines show the real and the imaginary part of the quasiclassical correlation function. Red and blue markers show the real and the imaginary part within the LHA approximation. The system-bath coupling parameter is $\xi = 0.6$. Left: correlation function for $\hat{A} = \hat{B} = \hat{s}^2$. Right, correlation function for $\hat{A} = \hat{B} = \hat{s}^3$. Top row, $\hbar\Omega\beta = 5$. Bottom row, $\hbar\Omega\beta = 0.4$.

5.1. Harmonic System Coupled to a Harmonic Bath. First we consider the special case of a quadratic system with potential function

$$V_0(\hat{s}) = \frac{1}{2}\Omega^2\hat{s}^2 \tag{5.5}$$

where $\Omega = 2$. In this case, we note that $V_0^{(n)}(s) = 0$ for all $n \geq 3$; thus the LHA is exact for all correlation functions.

The thermal Wigner density was obtained using the ASW procedure,[21,22] with a switching time of 30 system oscillation periods. The uncoupled harmonic system and harmonic bath were used to construct the zeroth order Hamiltonian. The ZPE of this zeroth Hamiltonian was used in the rescaling procedure. Figure 5 shows the position autocorrelation function, $C(t) = \langle s(0)s(t)\rangle$ of the system coordinate, as obtained from the procedure described in this paper with the LHA treatment, along with results obtained by diagonalizing the system-bath Hamiltonian at an inverse temperature, $\hbar\Omega\beta = 5$, at two values of system-bath coupling characterized by $\xi = 0.6$ and 1.2. As expected, the LHA quasiclassical results match the exact quantum results for this overall quadratic Hamiltonian. Also shown is the purely classical autocorrelation function. The latter has no imaginary part, and its real part differs substantially from the correct values. These differences are a consequence of sizable ZPE in the system-bath distribution, which are corrected by proper quantization of the density.

5.2. Anharmonic System. As a final example, we consider an anharmonic system with the following potential function

$$\hat{V}_0(s) = \frac{1}{2}\Omega^2\hat{s}^2 - 0.2\hat{s}^3 + 0.2\hat{s}^4 \tag{5.6}$$

with $\Omega = 2$. In the present case, the LHA is not the equivalent to the full quasiclassical correlation function. In Figures 6 and 7, we report the full quasiclassical autocorrelation functions for $\hat{A} = \hat{s}^2$ and $\hat{A} = \hat{s}^3$ at a low and a high temperature (corresponding to $\hbar\Omega\beta = 5$ and $\hbar\Omega\beta = 0.4$) using the procedure described in this

DOI: 10.1021/acs.jcim.9b00081
J. Chem. Inf. Model. 2019, 59, 2165−2174

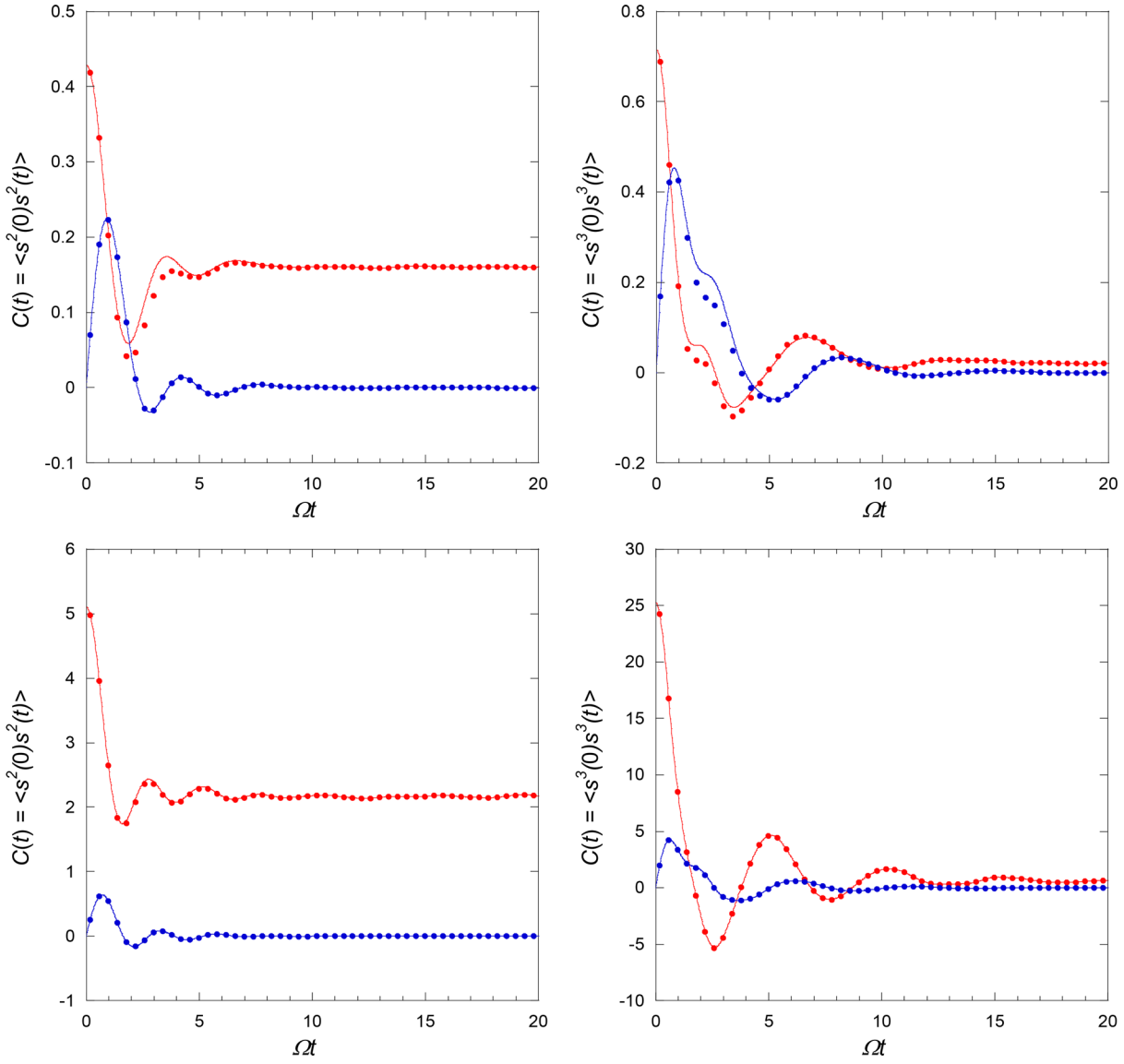

Figure 7. Correlation functions of harmonic system coupled to a harmonic bath. The red and blue lines show the real and the imaginary part of the quasiclassical correlation function. Red and blue markers show the real and the imaginary part within the LHA approximation. The system-bath coupling parameter is $\xi = 1.2$. Left, correlation function for $\hat{A} = \hat{B} = \hat{s}^2$. Right, correlation function for $\hat{A} = \hat{B} = \hat{s}^3$. Top row, $\hbar\Omega\beta = 5$. Bottom row, $\hbar\Omega\beta = 0.4$.

paper, along with the approximate LHA results. The initial Wigner distribution was generated using ASW, with the zeroth order part given by the quadratic part of the system-bath Hamiltonian.

Because of the strong asymmetry of the system potential, which is very pronounced at high temperature and also at low temperature because of the large zero-point energy of the system-bath Hamiltonian, the equilibrium averages and long-time values of the correlation functions are not equal to zero. In sharp contrast to the bare system dynamics discussed in section 4, the LHA is seen to reproduce the full quasiclassical correlation functions rather faithfully in all regimes, even with highly nonlinear operators. This is particularly encouraging for application to polyatomic systems.

6. CONCLUDING REMARKS

Quasiclassical calculations of correlation functions offer an efficient and often reasonably accurate simulation tool for condensed phase and biological processes. However, since many systems contain high-frequency vibrations, zero-point energy and quantum dispersion are quite prominent, requiring quantization of the phase space distribution.

The correct quasiclassical expression involves the Wigner–Weyl transform of the density multiplied by the first probed operator, which is a more demanding task than the calculation of the bare Wigner density. In this paper, we have described a procedure that samples trajectories from the Wigner phase space distribution, without sacrificing accuracy. This was done by accounting for the first operator in the dynamics, using properties of the stability matrix to obtain the required derivatives. We also described a local harmonic approximation that simplifies the expression, significantly reducing the number of differential equations that must be solved.

Test applications of the method to linear and nonlinear correlation functions in a one-dimensional anharmonic potential and a system-bath Hamiltonian showed that the method is

DOI: 10.1021/acs.jcim.9b00081
J. Chem. Inf. Model. 2019, 59, 2165−2174

relatively easy to implement. The LHA approximation gave overall good results, although it failed for one of the nonlinear correlation functions of the one-dimensional system. However, the LHA results were nearly quantitative in all test calculations on a system-bath Hamiltonian, at both high and low temperature and for weak or strong system-bath coupling strength. This success suggests that the method developed in this paper can be used in conjunction with the LHA approximation in calculations involving many degrees of freedom. As such, we hope that this approach will find utility in classical trajectory simulations of condensed-phase and biological phenomena.

APPENDIX

Here we give the differential equations for the trajectory derivatives for the case of the system-bath Hamiltonian considered in section 5.

The first-order derivatives are obtained from the $2(n+1) \times 2(n+1)$ stability matrix and are found to satisfy the differential equations

$$\begin{aligned}
\frac{\mathrm{d}}{\mathrm{d}t}\frac{\partial s}{\partial p_0} &= \frac{\partial p}{\partial p_0}\\
\frac{\mathrm{d}}{\mathrm{d}t}\frac{\partial Q_j}{\partial p_0} &= \frac{\partial P_j}{\partial p_0}\\
\frac{\mathrm{d}}{\mathrm{d}t}\frac{\partial p}{\partial p_0} &= -\frac{\partial^2 V}{\partial s^2}\frac{\partial s}{\partial p_0} - \sum_j \frac{\partial^2 V}{\partial s \partial Q_j}\frac{\partial Q_j}{\partial p_0}\\
&= -V_0''(s)\frac{\partial s}{\partial p_0} + \sum_j c_j \frac{\partial Q_j}{\partial p_0}\\
\frac{\mathrm{d}}{\mathrm{d}t}\frac{\partial P_j}{\partial p_0} &= -\frac{\partial^2 V}{\partial Q_j^2}\frac{\partial Q_j}{\partial p_0} - \sum_j \frac{\partial^2 V}{\partial s \partial Q_j}\frac{\partial s}{\partial p_0}\\
&= -\omega_j^2 \frac{\partial Q_j}{\partial p_0} + \sum_j c_j \frac{\partial s}{\partial p_0}
\end{aligned} \tag{6.1}$$

where V is the total system-bath potential. Equation 6.1 is solved with the following initial conditions

$$\left.\frac{\partial s}{\partial p_0}\right|_{t=0} = 0, \quad \left.\frac{\partial X_j}{\partial p_0}\right|_{t=0} = 0, \quad \left.\frac{\partial p}{\partial p_0}\right|_{t=0} = 1, \quad \left.\frac{\partial P_j}{\partial p_0}\right|_{t=0} = 0 \tag{6.2}$$

Differentiating eq 6.1 with respect to p_0 we obtain the following equations for the second derivatives,

$$\begin{aligned}
\frac{\mathrm{d}}{\mathrm{d}t}\frac{\partial^2 s}{\partial p_0^2} &= \frac{\partial^2 p}{\partial p_0^2}\\
\frac{\mathrm{d}}{\mathrm{d}t}\frac{\partial^2 X_j}{\partial p_0^2} &= \frac{\partial^2 P_j}{\partial p_0^2}\\
\frac{\mathrm{d}}{\mathrm{d}t}\frac{\partial^2 p}{\partial p_0^2} &= -V'''(s)\left(\frac{\partial s}{\partial p_0}\right)^2 - V''(s)\frac{\partial^2 s}{\partial p_0^2} + \sum_j c_j \frac{\partial^2 X_j}{\partial p_0^2}\\
\frac{\mathrm{d}}{\mathrm{d}t}\frac{\partial^2 P_j}{\partial p_0^2} &= -\omega_j^2 \frac{\partial^2 X_j}{\partial p_0^2} + \sum_j c_j \frac{\partial^2 s}{\partial p_0^2}
\end{aligned} \tag{6.3}$$

Higher order derivatives can be similarly generated. Using eq 6.3 gives the full quasiclassical correlation function. The LHA simplifies the higher order derivatives of the stability matrix to the form

$$\begin{aligned}
\frac{\mathrm{d}}{\mathrm{d}t}\frac{\partial^n s}{\partial p_0^n} &= \frac{\partial^n p}{\partial p_0^n}\\
\frac{\mathrm{d}}{\mathrm{d}t}\frac{\partial^n Q_j}{\partial p_0^n} &= \frac{\partial^n P_j}{\partial p_0^n}\\
\frac{\mathrm{d}}{\mathrm{d}t}\frac{\partial^n p}{\partial p_0^n} &= -V^{(n)}(s)\frac{\partial^n s}{\partial p_0^n} + \sum_j c_j \frac{\partial^n Q_j}{\partial p_0^n}\\
\frac{\mathrm{d}}{\mathrm{d}t}\frac{\partial^n P_j}{\partial p_0^n} &= -\omega_j^2 \frac{\partial^n Q_j}{\partial p_0^n} + \sum_j c_j \frac{\partial^n s}{\partial p_0^n}
\end{aligned} \tag{6.4}$$

AUTHOR INFORMATION

Corresponding Author

*E-mail: nmakri@illinois.edu.

ORCID

Amartya Bose: 0000-0003-0685-5096

Nancy Makri: 0000-0002-3310-7328

Notes

The authors declare no competing financial interest.

ACKNOWLEDGMENTS

This material is based upon work supported by the National Science Foundation under Award CHE-1665281.

REFERENCES

(1) Husimi, K. Some formal properties of the density matrix. *P. Phys. Math. Soc. Jpn.* **1940**, *22*, 264.

(2) Makri, N.; Thompson, K. Semiclassical influence functionals for quantum systems in anharmonic environments. *Chem. Phys. Lett.* **1998**, *291*, 101−109.

(3) Shao, J.; Makri, N. Forward-backward semiclassical dynamics with linear scaling. *J. Phys. Chem. A* **1999**, *103*, 9479−9486.

(4) Makri, N.; Nakayama, A.; Wright, N. Forward-backward semiclassical simulation of dynamical properties in liquids. *J. Theor. Comput. Chem.* **2004**, *3*, 391−417.

(5) Sun, X.; Miller, W. H. Forward-backward initial value representation for semiclassical time correlation functions. *J. Chem. Phys.* **1999**, *110*, 6635−6644.

DOI: 10.1021/acs.jcim.9b00081
J. Chem. Inf. Model. 2019, 59, 2165−2174

(6) Skinner, D. E.; Miller, W. H. Application of the forward-backward initial value representation for molecular energy transfer. *J. Chem. Phys.* **1999**, *111*, 10787−10793.
(7) Miller, W. H. The semiclassical initial value representation: a potentially practical way for adding quantum effects to classical molecular dynamics simulations. *J. Phys. Chem. A* **2001**, *105*, 2942−2955.
(8) Weyl, H. Quantenmechanik und Gruppentheorie. *Eur. Phys. J. A* **1927**, *46*, 1.
(9) Wigner, E. J. Calculation of the Rate of Elementary Association Reactions. *J. Chem. Phys.* **1937**, *5*, 720.
(10) Heller, E. J.; Brown, R. C. Errors in the Wigner approach to quantum dynamics. *J. Chem. Phys.* **1981**, *75*, 1048−1050.
(11) Wang, H.; Sun, X.; Miller, W. H. Semiclassical approximations for the calculation of thermal rate constants for chemical reactions in complex molecular systems. *J. Chem. Phys.* **1998**, *108*, 9726−9736.
(12) Sun, X.; Wang, H.; Miller, W. H. Semiclassical theory of electronically nonadiabatic dynamics: Results of a linearized approximation to the initial value representation. *J. Chem. Phys.* **1998**, *109*, 7064−7074.
(13) Miller, W. H. Generalization of the linearized approximation to the semiclassical initial value representation for reactive flux correlation functions. *J. Phys. Chem. A* **1999**, *103*, 9384−9387.
(14) Poulsen, J. A.; Nyman, G.; Rossky, P. J. Practical evaluation of condensed phase quantum correlation functions: A Feynman–Kleinert variational linearized path integral method. *J. Chem. Phys.* **2003**, *119*, 12179−12193.
(15) Metropolis, N.; Rosenbluth, A. W.; Rosenbluth, M. N.; Teller, H.; Teller, E. Equation of state calculations by fast computing machines. *J. Chem. Phys.* **1953**, *21*, 1087−1092.
(16) Shi, Q.; Geva, E. Semiclassical theory of vibrational energy relaxation in the condensed phase. *J. Phys. Chem. A* **2003**, *107*, 9059−9069.
(17) Frantsuzov, P. A.; Neumaier, A.; Mandelshtam, V. A. Gaussian resolutions for equilibrium density matrices. *Chem. Phys. Lett.* **2003**, *381*, 117.
(18) Frantsuzov, P. A.; Mandelshtam, V. A. Quantum statistical mechanics with Gaussians: Equilibrium properties of van der Waals clusters. *J. Chem. Phys.* **2004**, *121*, 9247.
(19) Heller, E. J. Time-dependent variational approach to semiclassical dynamics. *J. Chem. Phys.* **1976**, *64*, 63−73.
(20) Shao, J.; Pollak, E. A new time evolving Gaussian series representation of the imaginary time propagator. *J. Chem. Phys.* **2006**, *125*, 133502.
(21) Bose, A.; Makri, N. Evaluation of the Wigner distribution via classical adiabatic switching. *J. Chem. Phys.* **2015**, *143*, 114114.
(22) Bose, A.; Makri, N. Wigner Distribution by Adiabatic Switching in Normal Mode or Cartesian Coordinates and Molecular Applications. *J. Chem. Theory Comput.* **2018**, *14*, 5446−5458.
(23) Montoya-Castillo, A.; Reichman, D. R. Path integral approach to the Wigner representation of canonical density operators for discrete systems coupled to harmonic baths. *J. Chem. Phys.* **2017**, *146*, 024107.
(24) Makri, N. Improved Feynman propagators on a grid and non-adiabatic corrections within the path integral framework. *Chem. Phys. Lett.* **1992**, *193*, 435−444.
(25) Bose, A.; Makri, N. Coherent State-Based Path Integral Methodology for Computing the Wigner Phase Space Distribution. *J. Phys. Chem. A* **2019**, submitted for publication.
(26) Caldeira, A. O.; Leggett, A. J. Path integral approach to quantum Brownian motion. *Phys. A* **1983**, *121*, 587−616.
(27) Makri, N. The linear response approximation and its lowest order corrections: an influence functional approach. *J. Phys. Chem. B* **1999**, *103*, 2823−2829.
(28) Walters, P. L.; Allen, T. C.; Makri, N. Direct determination of harmonic bath parameters from molecular dynamics simulations. *J. Comput. Chem.* **2017**, *38*, 110−115.

DOI: 10.1021/acs.jcim.9b00081
J. Chem. Inf. Model. 2019, 59, 2165−2174